OCEANOGRAPHY

Tipping points of Mississippi Delta marshes due to accelerated sea-level rise

Torbjörn E. Törnqvist[1]*, Krista L. Jankowski[1†], Yong-Xiang Li[1,2], Juan L. González[1,3]

Coastal marshes are threatened by relative sea-level (RSL) rise, yet recent studies predict marsh survival even under the high rates of RSL rise expected later in this century. However, because these studies are mostly based on short-term records, uncertainty persists about the longer-term vulnerability of coastal marshes. We present an 8500-year-long marsh record from the Mississippi Delta, showing that at rates of RSL rise exceeding 6 to 9 mm year^{-1}, marsh conversion into open water occurs in about 50 years. At rates of RSL rise exceeding ~3 mm year^{-1}, marsh drowning occurs within a few centuries. Because present-day rates of global sea-level rise already surpass this rate, submergence of the remaining ~15,000 km^2 of marshland in coastal Louisiana is probably inevitable. RSL-driven tipping points for marsh drowning vary geographically, and those for the Mississippi Delta may be lower than elsewhere. Nevertheless, our findings highlight the need for consideration of longer time windows in determining the vulnerability of coastal marshes worldwide.

INTRODUCTION

Landscapes and ecosystems are known to respond in a nonlinear fashion to external stresses (*1*). Coastal wetlands represent a family of ecosystems that are prone to potentially irreversible collapse because of this mechanism. For example, the productivity of a common coastal marsh grass (*Spartina alterniflora*) peaks in a distinct elevation range defined by tide levels (*2*). As a consequence, persistent submergence at a level that exceeds this range (and absent abundant sediment to offset this) will lead to rapid degradation and the conversion of marsh into tidal flat or open water, representing alternative stable states as predicted theoretically (*3*).

Coastal marshes are among the most valuable ecosystems on the planet (*4*), yet there is widespread concern about their sustainability due to accelerated sea-level rise and other human-induced stresses. They generally form in the upper half of the intertidal zone and are the result of a delicate balance between vertical accretion and relative sea-level (RSL) rise, driven by a host of physical (e.g., tidal inundation), biological (e.g., plant productivity), and chemical (e.g., decomposition) processes (*5–7*). Because landward migration of coastal wetlands is increasingly hampered owing to human interference or steep upland slopes (*8*), marsh survival depends, to a large extent, on surface-elevation gain. However, several studies have shown that even with substantial accretion rates, marshes may be subject to degradation due to sediment compaction (*9*, *10*).

An ensemble of numerical models (*11*) suggests that threshold rates of RSL rise for marsh survival (generally 10 to 50 mm year^{-1}) are determined mainly by tidal range and suspended sediment concentration (SSC). As a result, several recent studies have advanced the view that marshes may be relatively resilient (*12*), but inferences like these are, to a large extent, based on observations over annual to decadal time scales only (*13*).

The Mississippi Delta (MD) experiences some of the highest rates of coastal wetland loss in the world (*14*). A recent analysis of wetland change at 185 sites across the MD has shown that, over the past decade, vertical accretion has kept pace with the rate of RSL rise (13 ± 9 mm year^{-1}, determined with respect to the wetland surface) at about 65% of these sites (*10*). However, it remains largely unknown to what extent coastal marshes are sustainable over longer (i.e., multidecadal to centennial) time scales when sediment compaction, ponding, and erosion become significant. The high rates of present-day RSL rise in the MD are not unusual. For example, comparable rates are seen in the Po Delta (*15*), and even higher rates occur in the Mekong Delta (*16*). Here, we test the hypothesis that marshes in the MD can keep pace with rates of RSL rise up to 10 mm year^{-1} by considering marsh records that stretch much of the Holocene. While this empirical approach cannot disentangle all the relevant ecogeomorphic processes and nonlinear feedbacks, it offers direct observational evidence on how their interplay determines marsh survival in the long term.

RESULTS

A high-resolution RSL record for the MD that covers the past 8.5 ka (*17*) (Fig. 1 and Materials and Methods), combined with detailed facies descriptions from the associated boreholes that were drilled to carry out the sea-level reconstruction (Figs. 2 and 3 and Materials and Methods), enables the evolution of paleo-marshes to be tied directly to rates of RSL rise as determined with respect to the preexisting land surface. The RSL record is based on 72 sea-level index points (SLIPs) derived from compaction-free basal marsh peat—the organic-rich facies that immediately overlie a transgressive wetland paleosol on top of a highly consolidated substrate. Further details about the methodology for sea-level reconstruction can be found elsewhere (*18*).

Rates of RSL rise (Fig. 1) approach 10 mm year^{-1} during the earliest phase of the record and then progressively decrease to ~0.5 mm year^{-1} during the preindustrial millennium (*19*). As a result, this record enables us to study paleo-marsh response to a wide range of rates of RSL rise as determined with respect to the preexisting land surface. The early portion of the RSL record captures rates predicted

[1]Department of Earth and Environmental Sciences, Tulane University, 6823 St. Charles Avenue, New Orleans, LA 70118-5698, USA. [2]Key Laboratory of Surficial Geochemistry (Ministry of Education), School of Earth Sciences and Engineering, Nanjing University, Nanjing 210046, China. [3]School of Earth, Environmental and Marine Sciences, University of Texas–Rio Grande Valley, Edinburg, TX 78539, USA.
*Corresponding author. Email: tor@tulane.edu
†Present address: Coastal Protection and Restoration Authority, 150 Terrace Avenue, Baton Rouge, LA 70802, USA.

worldwide for the latter part of the 21st century under the RCP4.5 and RCP8.5 emission scenarios (*20*).

The stratigraphic analysis focused initially on the 72 sites from which SLIPs were obtained; 15 representative sedimentary logs (10 of which from SLIP sites) are illustrated in Fig. 3. While they mostly feature muddy, organic-rich marsh facies that immediately overlie the paleosol, the subsequent succession varies widely. Specifically, before ~6.8 ka BP (before present; defined as 1950 Common Era), a transition from marsh to lagoonal (i.e., open water) facies with characteristic fauna (commonly the brackish water clam *Rangia cuneata*) is nearly always present. In contrast, the subsequent portion of the record (<6.8 ka BP) mostly lacks indicators of open-water conditions. Instead, terrestrial facies (predominantly marsh or swamp mud, i.e., including freshwater successions) persist, indicating that vertical
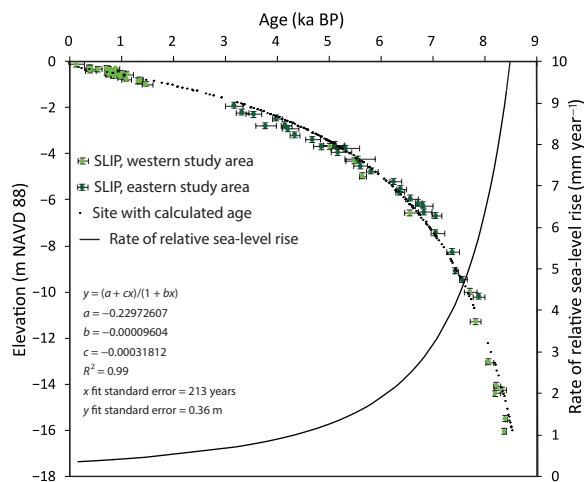
accretion kept pace with, or exceeded, the rate of RSL rise. It is important to note that boreholes with comparable basal ages in western and eastern (Fig. 2) portions of the MD exhibit a notably similar stratigraphy (Fig. 3 and figs. S1 and S2).

The analysis was extended by 283 additional boreholes that feature a stratigraphically similar transition (see Supplementary Spreadsheet). Just as the logs discussed above, these sites are scattered more than 100 km apart across the MD and derive from the two study areas that measure 25 to 40 km across (Fig. 2). Because of the large number of observations, spatial variability that inevitably affects smaller areas is therefore filtered out, and the data enable us to extract the broader patterns that characterize this region. Nevertheless, it should be noted that, when examined in more detail, the stratigraphy exhibits a rich variability. This is illustrated by sites with multiple episodes of drowning and return to terrestrial conditions (Fig. 3), demonstrating that other factors, such as the proximity to a sediment source, can be locally important. Each of the borehole logs was classified into fully terrestrial versus drowned facies successions, with the latter (fig. S3) subdivided into gradual or rapid drowning (table S2). About 6.5% of the logs lacked the detail to confidently classify them and were recorded as inconclusive.

Given the tight age-depth relationship (Fig. 1), ages can be assigned to the facies transition at the top of the paleosol in undated boreholes within ~200-year error, enabling the rate of RSL rise with respect to the preexisting land surface to be estimated for each site. The results (Fig. 4) show that when rates are <2 mm year^{-1}, facies successions are always terrestrial. Above this rate, the first drowned sites are encountered. Only when rates of RSL rise exceed 3 mm year^{-1} does drowning occur in at least 80% of the sites; a small proportion (<10%) remained terrestrial throughout the Holocene. This indicates that, even when rates of RSL rise are very high, local conditions (most likely proximity to a major sediment source) may prevent drowning, but the point is that such conditions are rare. Our findings are robust when viewed separately for the two study areas (fig. S4) or when only relatively thick basal marsh successions are considered (fig. S5), indicating that a rate of RSL rise of 3 mm year^{-1} represents a threshold rate for marsh drowning in the MD, regardless of marsh maturity.

Before 8.2 ka BP, when rates of RSL rise exceeded 6 to 9 mm year^{-1}, basal marsh facies have a median thickness of only 15 cm (Fig. 3 and Table 1), even after sites with erosional transitions are removed. We refer to these thin strata as incipient marshes (or fringing marshes) with widths of a few kilometers or less, taking into account their
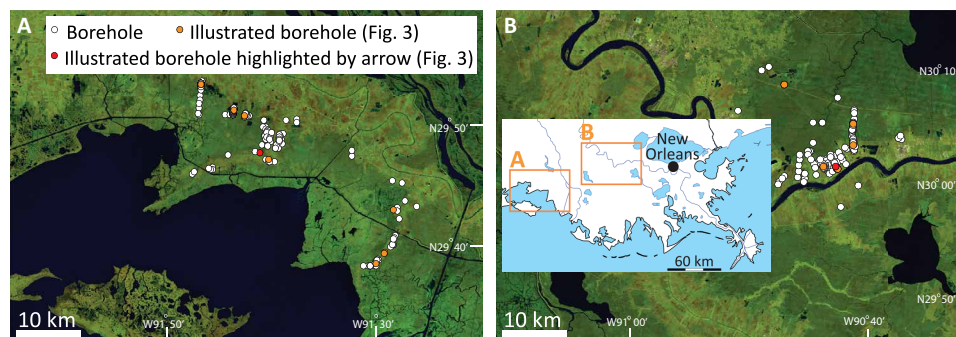

Fig. 1. RSL curve and rate of RSL rise in the MD. A total of 72 sea-level index points (SLIPs) from basal marsh peat provides the Holocene RSL history with respect to the compaction-free, (mostly) Pleistocene basement. The location of the study areas is shown in Fig. 2. The gap between ~3.0 and 1.5 ka BP (before present) is merely due to the fact that this time interval was not sampled for ^{14}C dating; it should not be interpreted as a phase with a rate of RSL rise that deviates from the long-term trend. Note also that the youngest SLIP predates the global sea-level acceleration of the past century (not shown in this record). All other (non-SLIP) data points are shown by means of the small black symbols that elucidate the shape of the function that was fitted to the SLIP data. The first derivative of the RSL curve exhibits rates of RSL rise between 8.5 and 0.15 ka BP.

Fig. 2. Distribution of the 355 boreholes across the MD that were used for the paleo-marsh analysis. Note that the distance between the two study areas (**A** and **B**) is about 100 km and that boreholes within these two regions are scattered up to 40 km apart. This circumvents sampling bias associated with local conditions that may not be representative for a wider region. The location of the 15 boreholes illustrated in Fig. 3 is shown in orange or red. Base map data: Google, SIO, NOAA, U.S. Navy, NG, GEBCO, Landsat/Copernicus, Terrametrics.
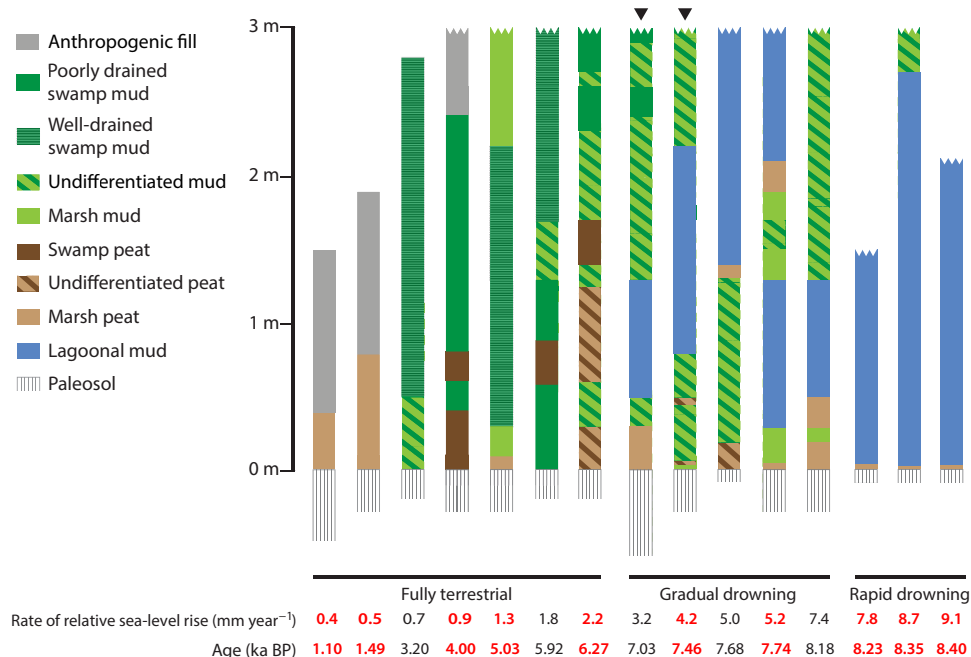
Fig. 3. Characteristic transgressive facies successions from the past 8500 years. A selection of 15 representative sedimentary logs features the transition from a wetland paleosol to basal Holocene facies and the overlying succession (details about facies units are provided in table S1). For ease of comparison, the logs have been adjusted vertically to align the top of the paleosol and arranged with increasing age (and depth) from left to right [in reality, the elevation of the top of the paleosol decreases from ~0.5 to 16 m below North American Vertical Datum of 1988 (NAVD 88); see Supplementary Spreadsheet]. The serrated pattern is used for logs that do not extend all the way to the land surface. For each log, the weighted mean calibrated age (in ka BP) of the basal facies that drape the paleosol and the rate of RSL rise (the first derivative of the equation in Fig. 1) is provided. Directly dated cores are indicated in red; for the other cores, the age of the basal Holocene facies was calculated by means of the equation in Fig. 1. Note that the two logs marked by arrows with largely similar stratigraphy are ~100 km apart (all core locations are shown in Fig. 2). Additional sedimentary logs are shown for the western and eastern study areas separately in figs. S1 and S2.
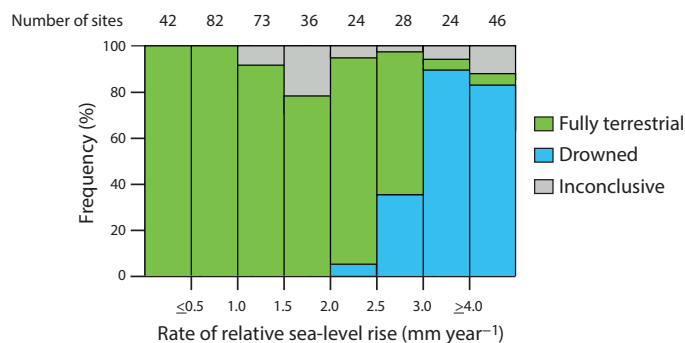

Fig. 4. Relationship between the rate of RSL rise and marsh persistence. The relative proportion of facies successions (table S2) is determined for eight increments of rates of RSL rise to identify the tipping point for marsh drowning. The abrupt increase in the proportion of drowned sites between 2.5 and 3.0 mm year^{-1} illustrates the nonlinear nature of the marsh response to the rate of RSL rise. Similar plots are shown for the western and eastern study areas separately (fig. S4) and for basal marsh successions ≥50 cm thick (fig. S5).

original (decompacted) thickness of typically <50 cm (Table 1) and an average seaward slope of the preexisting land surface (i.e., the Pleistocene basement) of about 0.00025 (*21*). Clearly, these incipient marshes differed strongly from the extensive marshlands that formed later during the Holocene; in addition to the fact that they never fully developed, they occupied a much smaller area. The incipient marshes exhibit rapid drowning, as opposed to the gradual

drowning that is more common at sites within the 6.8 to 8.2 ka BP time window where the median thickness of basal marsh facies is 30 to 50 cm (Table 1). While incipient marshes could start to form even under the highest rates of RSL rise seen in our record, they also quickly collapsed.

The duration of marsh persistence for the sites that eventually flooded can be estimated from the thickness of the drowned marsh facies, assuming that vertical accretion initially kept pace with the rate of RSL rise and using a reduction in thickness by a factor of 2.5 due to compaction (*22*). This estimate suggests (Table 1) that drowning of the incipient marshes before 8.2 ka BP typically occurred in ~50 years or less, while between 8.2 and 6.8 ka BP marshes were able to persist ~300 years on average.

DISCUSSION AND IMPLICATIONS

To what extent is early Holocene marsh evolution relevant to present-day and future conditions? Before the embankment of distributaries and the resulting isolation of the delta plain from clastic sediment input, MD marshes likely enjoyed relatively high SSC values. This is suggested by present-day measurements of up to 150 mg liter^{-1} during the 2011 flood in Atchafalaya Bay (*23*)—a setting representative of the large, diffuse plumes associated with the shallow-water lobes that dominated the Holocene MD. However, because of extensive damming in the drainage basin (*24*), the present-day sediment supply from the Mississippi River is likely lower than it was during the early Holocene. In other words, despite presumably higher sediment availability than the presently observed SSC values, our analysis shows

Table 1. Thickness and estimated life span of drowned marsh facies.

	Drowned marsh facies—all sites*			Drowned marsh facies—selected sites†		
	Median (mean) thickness (m)	Median (mean) life span (years)‡	Number of observations	Median (mean) thickness (m)	Median (mean) life span (years)‡	Number of observations
Mostly gradual drowning (after 8.2 ka BP)	0.30 (0.43)	212 (282)§	51	0.50 (0.58)	310 (372)§	25
Mostly rapid drowning (before 8.2 ka BP)	0.10 (0.18)	25 (50)	17	0.15 (0.34)	46 (98)	8

*All sites ($n = 68$) that feature lagoonal facies, including those where the contact between terrestrial (usually marsh) and lagoonal facies is erosional.   †Selected sites ($n = 33$) where the terrestrial to lagoonal facies contact is less likely to be erosional.   ‡Estimated by correcting the thickness for compaction (a factor of 2.5) and assuming that the accretion rate approximately tracked the rate of RSL rise at the onset of marsh formation.   §Note that mean values always exceed median values (typically due to one or a few sites with relatively large numbers); therefore, median values are used in the interpretation.

that early Holocene marshes were unable to keep pace with RSL rise. The microtidal range in this region (presently <0.5 m) limits marsh resilience, but the tidal range was likely higher before 8 ka BP [it has been comparable to the present-day tidal regime since that time (*25*)]. On the other hand, early Holocene atmospheric CO_2 concentrations were about 65% of present-day values. This may have reduced primary production rates and the organic contribution to marsh accretion (*26*). On balance, however, early Holocene conditions—a period with no detrimental human impacts—likely favored marsh resilience compared to the present day.

The short-term resilience of MD marshes is illustrated by the fact that they often keep up with the present-day rate of RSL rise of 13 ± 9 mm year^{-1}, as determined with respect to the wetland surface (see Materials and Methods), but this is based on time series that are only 6 to 10 years long (*10*). In contrast, the paleo-marsh record shows that such conditions are unsustainable over multidecadal to centennial time scales. While the empirical evidence for this is robust, a comprehensive understanding of the causes of this contrast will require more research. It is plausible that a suite of processes become increasingly important when rapid rates of RSL rise persist for longer than a few decades. This includes decomposition and compaction of the high-porosity, low-bulk density wetland sediments (~0.3 g cm^{-3} in modern MD marshes; table S3). Compaction is known to be a significant factor in the comparatively muddy (~30% organic-matter content; table S3) MD strata (*27, 28*) that experience relatively high effective stresses. Other processes that were likely significant during the rapid early Holocene RSL rise are ponding and pond expansion (*29*), as well as marsh-edge erosion by waves (*30*) that can evolve into a runaway process once initiated (*31*). This is reflected by the fact that about half of the drowned marshes in our dataset exhibit erosive surfaces (see Supplementary Spreadsheet). Last, the lack of elevation capital in the MD (table S3) also limits marsh resilience in the longer term.

Our findings differ markedly from recent modeling (*12*) that predicts the response of coastal wetlands worldwide to future RSL rise and concludes that these ecosystems may be unexpectedly resilient. We attribute this difference, at least in part, to the fact that the datasets that underpin such modeling studies cover short observational windows of typically decades or less (*11*) and therefore do not capture key long-term processes such as those mentioned above. For example, it is well known that accelerated RSL rise can trigger enhanced vertical accretion in the short term (*2*), but our findings show

that such phenomena are likely to be transient because of an inevitable accretion deficit.

We stress the importance of the rate of RSL rise as determined with respect to the preexisting land surface—as used in the present study—because it dictates whether or not marshes will eventually drown, and how soon drowning is likely to occur. Furthermore, rates of RSL rise as determined in this way permit comparison with globally averaged rates of sea-level rise. However, the specific threshold rates of RSL rise for the MD are not likely to be transferable to other coastal settings, given the dependence of marsh vulnerability on other factors, including—but not limited to—SSC and tidal range, as well as the ability of coastal marshes to migrate landward (*12*). This is illustrated, for example, by the considerably higher rates of RSL rise needed for marsh drowning in Great Britain (*32*). Furthermore, while the low-elevation MD marshes tend to convert into open water under rapid rates of RSL rise, in other settings with a higher tidal range, this may involve the transformation of high marsh into low marsh (*33*) or low marsh into tidal flat (*8*). Nevertheless, we hypothesize that a chief finding of the present study—the large disparity between marsh vulnerability over short versus long time scales—may be generally valid and that the existence of tipping points is a fundamental feature of these ecosystems. The implication of this would be that the associated threshold rates of RSL rise for coastal marsh sustainability may be lower than what studies based on instrumental records suggest. Testing this hypothesis by means of additional studies of paleo-marsh evolution should therefore be a priority for future research. Given the importance to capture the high rates of RSL rise that occurred during the early Holocene, we anticipate that the best targets for this purpose are other large deltas that are most likely to preserve records of this age.

Studies of a wide range of ecosystems have shown that reduced resilience (e.g., due to other, nonclimatic anthropogenic influences) renders them more prone to rapid transformation (*1*). The severe degradation of MD marshes due to a variety of human impacts, including the dissection of the area by over 15,000 km of canals (*14*), has already resulted in such a loss of resilience and will make a continued shift to open water more likely. The globally averaged rate of sea-level rise between 2006 and 2015 is 3.58 ± 0.48 mm year^{-1} (*20*), and even a best-case scenario in long-term global sea-level projections predicts rates of 5 to 6 mm year^{-1} for about 2000 years (*34*). We therefore conclude not only that the 3 mm year^{-1} threshold rate of RSL rise in the MD has already been crossed but also that this

condition is likely to persist far beyond the time scale of MD marsh drowning. In other words, drowning is inevitable, and conversion back to marsh will be unlikely. This is a major threat not only to one of the ecologically richest environments of the United States but also for the 1.2 million inhabitants (table S4) and associated economic assets that are surrounded by MD marshland. Our findings, viewed within the context of long-term sea-level projections, raise the question whether coastal marshes elsewhere may be more vulnerable than commonly recognized.

MATERIALS AND METHODS
RSL record
The RSL record was obtained entirely from compaction-free basal peats; paleoenvironments were inferred from $\delta^{13}C$ data (18), augmented with information from plant macrofossils (18) and foraminifera (35). Most of the basal peats formed in marshes with brackish to intermediate salinity, i.e., within the intertidal zone. The 72 SLIPs that form the basis for the RSL record were plotted with respect to North American Vertical Datum of 1988 (NAVD 88), in accordance with a previously published synthesis (17). The curve fitting software package TableCurve 2D, version 5.01.02 (www.sigmaplot.co.uk/products/tablecurve2d/tablecurve2d.php) was used to fit and rank 3665 equations to obtain the RSL curve using the central values of the SLIPs ("Sample elevation—base (m NAVD)" and "Calibrated age—weighted mean (cal yr BP)") (17). Because the Holocene RSL history of this region is dominated by glacial isostatic adjustment (peripheral bulge subsidence) as reflected by continuous but progressively decreasing rates of RSL rise (36), we only considered curves characterized by monotonic RSL rise. Subtle, century-scale RSL fluctuations with amplitudes of a few decimeters (19) likely existed, but would have a relatively small impact on the most important portion of our RSL record when rates of RSL rise were the highest (i.e., the effect would be limited to subtle accelerations and decelerations). RSL curves were graphically evaluated and assessed for goodness of fit (R^2) and the standard error between the data and the fitted curve. The RSL curve with optimal outcomes with respect to these criteria (Fig. 1) was used to calculate an estimated age of the base of the Holocene succession (i.e., the elevation of the top of the paleosol with respect to NAVD 88) at the 283 sites for which no direct ^{14}C dating was available (for the 72 sites with SLIPs, the calibrated ^{14}C age was used). The associated age error for the sites without direct dating is 213 years, which introduces some uncertainty in the rate of RSL rise at each site. This uncertainty has been accounted for in the inferred threshold rate for rapid marsh drowning (6 to 9 mm year^{-1}).

The rate of RSL rise as a function of time was obtained by means of the first derivative of the RSL curve (Fig. 1). This number is used to characterize the rate of RSL rise at the onset of marsh (or swamp) formation at each individual site. For drowned sites, the top of the marsh facies has a younger age and, thus, corresponds to slower rates of RSL rise as derived from this record, but given the slow decline of the rate of RSL rise, this is a minor issue. Around 8.2 ka BP, the time of the ~7.5 mm year^{-1} threshold rate of RSL rise between gradual and rapid marsh drowning, the rate of RSL rise decreases by ~0.3 mm year^{-1} between the base and the top of drowned marsh facies (based on the mean duration of marsh persistence of about 50 years). For the tipping point that defines the onset of gradual marsh drowning (3 mm year^{-1} around 6.9 ka BP), this value is ~0.5 mm year^{-1}, based on a mean time window for marsh drowning of 300 years.

Within this context, it is important to stress the fundamental difference between the Holocene RSL record from basal marsh facies (mostly basal peat) (Fig. 1) that exhibits rates with respect to the largely compaction-free Pleistocene basement (i.e., the preexisting land surface) and that was used to assess the vulnerability of marshes that formed immediately above this surface, versus present-day rates of RSL rise as determined with respect to the land surface (10). The former provides a robust record of RSL rise that is spatially uniform across the two study areas (Fig. 1). In contrast, the latter rates are much higher (13 ± 9 mm year^{-1}) and spatially variable owing to a combination of factors, including the climate-driven global acceleration of sea-level rise (37), subsurface fluid extraction (38), and high compaction rates (10, 27, 28).

Borehole data and facies analysis
The majority of the borehole data (n = 334) were collected by hand, by means of an Edelman auger and a 3-cm-diameter gouge (39). Sediments were described in the field in 10-cm increments, with particular attention to sediment texture, organic-matter content, plant and other fossil remains, color, oxidation state, and sedimentary structures. A smaller number (n = 21) of relatively deep boreholes (typically >12 m) were drilled with a Geoprobe (model 6610 DT) that produced 4-cm-diameter cores that were also described in the field, in a similar way. In many cases, multiple cores were collected at the same site to ascertain that the sampled sections had suffered minimal disturbance (35). No evidence was found for incomplete recovery or sediment compaction due to coring with the Geoprobe. Unlike the hand-drilled boreholes, Geoprobe cores only extended a few meters above the Pleistocene-Holocene transition and therefore only sampled the portion of the Holocene succession of particular interest to the present study.

Borehole data for this study were selected from a larger database that resides at Tulane University, based on the following criteria: (i) only boreholes from the MD were considered; (ii) a well-defined and conformable Pleistocene-Holocene transition (nearly always defined by a dark gray, immature paleosol) had to be present; and (iii) the overlying facies succession had to be at least ~2 m thick if it did not extend all the way to the land surface (thinner facies successions were only included if they showed evidence for drowning). This minimum length was chosen to ensure that at least ~400 years of record was captured. Nevertheless, we cannot rule out that lagoonal facies may occur above the section that was examined in a few of the boreholes drilled with the Geoprobe.

The spatial distribution of boreholes (Fig. 2) is associated with the paleogeography of the region during the early Holocene and covers most of the area where the Pleistocene occurs within about 15 m below present mean sea level. These are the only portions of the MD where meaningful paleo-marsh records can be obtained (i.e., those that can be tied directly to the compaction-free RSL record). The study areas are located on the flanks of a major paleovalley (40) that had been filled around the time when the first marsh facies in our record started to accumulate, reflecting lateral dispersal of sediment and initial delta formation, similar to what is seen around this time worldwide (41). Because the filled paleovalley was the nucleus for the emergence of the Holocene MD, it is unlikely that the study areas were isolated from the sediment source (i.e., the mouth of the Mississippi River). Nevertheless, since the shoreline must have migrated landward at a relatively rapid pace during the early Holocene, we cannot rule out the possibility that our study areas were sufficiently

far seaward from the river mouth to experience a temporary period of reduced sediment supply. However, it is important to stress that shoreline retreat followed by delta progradation was fundamentally driven by the rapid reduction in the rate of RSL rise (Fig. 1). In other words, any possible changes in local sediment delivery were dictated by changes in the rate of RSL rise. We also stress that the possible role of a temporary reduction in sediment supply due to shoreline retreat remains to be tested because the exact position of the shoreline of maximum transgression in this region is not well constrained.

The facies classification (table S1) builds on previous studies (42–45) with slight modifications. In several cases, the borehole descriptions lacked the detail to confidently enable facies identification, which led to a portion of the sediments being classified as undifferentiated mud or peat. The main implication of this uncertainty is that some lagoonal muds may have been missed, including in shallower cores than the age-depth range in which lagoonal muds are common (Fig. 3 and figs. S1 and S2). Since the interpretation relies heavily on the identification of these open-water facies, they were only classified as such when there was high confidence in their recognition. In other words, the interpretation was carried out with caution, and we can therefore not rule out the possibility that more lagoonal facies occur, including in boreholes with rates of RSL rise <3 mm year^{-1} with respect to the preexisting land surface. The implication of this is that the inferred tipping points are conservative; i.e., threshold rates of RSL rise could be even somewhat lower.

A critical element of the facies analysis is the transition zone that includes the wetland paleosol (which, in turn, rests on highly consolidated Pleistocene strata) and the overlying Holocene succession. Here, we offer some additional details about this transition zone, focusing particularly on the older portion of the record that exhibits marsh drowning. The wetland paleosol has been classified as an Entisol, suborder Aquent (18, 46), characterized by highly decomposed organic matter that accumulated in a waterlogged environment. Paleoenvironmental analyses (18, 35) have shown that in the oldest portion of the record, this paleosol formed in the intertidal zone. An extensive ^{14}C study of this paleosol and peat from an overlying incipient marsh (47) shows that the peat, despite a thickness of only a few centimeters, contains datable plant macrofossils, unlike the underlying paleosol that was dated by ramped pyrolysis/oxidation ^{14}C analysis. The ^{14}C dating indicates that the age difference between the paleosol and the incipient marsh is within the error margins of the ^{14}C data. We interpret this transgressive succession [illustrated photographically in (18)] as one that consists initially of a nascent, intertidal wetland that pedogenically altered the preexisting substrate but exhibited limited vertical accretion (i.e., the paleosol) before the transformation into an incipient and vertically accreting, organic-rich deposit (i.e., the marsh). This succession is comparable to modern, permanently waterlogged dark gray soils that develop in newly formed *S. alterniflora* marshes that also feature a thin, brownish, organic-rich unit near the top, similar to our incipient marsh. These soils take as long as a century to evolve into fully developed, organic-rich marsh soils (48).

SUPPLEMENTARY MATERIALS

Supplementary material for this article is available at http://advances.sciencemag.org/cgi/content/full/6/21/eaaz5512/DC1

REFERENCES AND NOTES

1. M. Scheffer, S. Carpenter, J. A. Foley, C. Folke, B. Walker, Catastrophic shifts in ecosystems. *Nature* **413**, 591–596 (2001).
2. J. T. Morris, P. V. Sundareshwar, C. T. Nietch, B. Kjerfve, D. R. Cahoon, Responses of coastal wetlands to rising sea level. *Ecology* **83**, 2869–2877 (2002).
3. M. Marani, A. D'Alpaos, S. Lanzoni, L. Carniello, A. Rinaldo, Biologically-controlled multiple equilibria of tidal landforms and the fate of the Venice lagoon. *Geophys. Res. Lett.* **34**, L11402 (2007).
4. R. Costanza, R. d'Arge, R. de Groot, S. Farber, M. Grasso, B. Hannon, K. Limburg, S. Naeem, R. V. O'Neill, J. Paruelo, R. G. Raskin, P. Sutton, M. van den Belt, The value of the world's ecosystem services and natural capital. *Nature* **387**, 253–260 (1997).
5. S. Fagherazzi, M. L. Kirwan, S. M. Mudd, G. R. Guntenspergen, S. Temmerman, A. D'Alpaos, J. van de Koppel, J. M. Rybczyk, E. Reyes, C. Craft, J. Clough, Numerical models of salt marsh evolution: Ecological, geomorphic, and climatic factors. *Rev. Geophys.* **50**, RG1002 (2012).
6. M. L. Kirwan, J. P. Megonigal, Tidal wetland stability in the face of human impacts and sea-level rise. *Nature* **504**, 53–60 (2013).
7. D. M. FitzGerald, Z. Hughes, Marsh processes and their response to climate change and sea-level rise. *Annu. Rev. Earth Planet. Sci.* **47**, 481–517 (2019).
8. K. Thorne, G. MacDonald, G. Guntenspergen, R. Ambrose, K. Buffington, B. Dugger, C. Freeman, C. Janousek, L. Brown, J. Rosencranz, J. Holmquist, J. Smol, K. Hargan, J. Takekawa, U.S. Pacific coastal wetland resilience and vulnerability to sea-level rise. *Sci. Adv.* **4**, eaao3270 (2018).
9. D. R. Cahoon, D. J. Reed, J. W. Day Jr., Estimating shallow subsidence in microtidal salt marshes of the southeastern United States: Kaye and Barghoorn revisited. *Mar. Geol.* **128**, 1–9 (1995).
10. K. L. Jankowski, T. E. Törnqvist, A. M. Fernandes, Vulnerability of Louisiana's coastal wetlands to present-day rates of relative sea-level rise. *Nat. Commun.* **8**, 14792 (2017).
11. M. L. Kirwan, S. Temmerman, E. E. Skeehan, G. R. Guntenspergen, S. Fagherazzi, Overestimation of marsh vulnerability to sea level rise. *Nat. Clim. Chang.* **6**, 253–260 (2016).
12. M. Schuerch, T. Spencer, S. Temmerman, M. L. Kirwan, C. Wolff, D. Lincke, C. J. McOwen, M. D. Pickering, R. Reef, A. T. Vafeidis, J. Hinkel, R. J. Nicholls, S. Brown, Future response of global coastal wetlands to sea-level rise. *Nature* **561**, 231–234 (2018).
13. R. W. Parkinson, C. Craft, R. D. DeLaune, J. F. Donoghue, M. Kearney, J. F. Meeder, J. Morris, R. E. Turner, Marsh vulnerability to sea-level rise. *Nat. Clim. Chang.* **7**, 756 (2017).
14. J. W. Day Jr., D. F. Boesch, E. J. Clairain, G. P. Kemp, S. B. Laska, W. J. Mitsch, K. Orth, H. Mashriqui, D. J. Reed, L. Shabman, C. A. Simenstad, B. J. Streever, R. R. Twilley, C. C. Watson, J. T. Wells, D. F. Whigham, Restoration of the Mississippi Delta: Lessons from Hurricanes Katrina and Rita. *Science* **315**, 1679–1684 (2007).
15. P. Teatini, L. Tosi, T. Strozzi, Quantitative evidence that compaction of Holocene sediments drives the present land subsidence of the Po Delta, Italy. *J. Geophys. Res.* **116**, B08407 (2011).
16. C. Zoccarato, P. S. J. Minderhoud, P. Teatini, The role of sedimentation and natural compaction in a prograding delta: Insights from the mega Mekong delta, Vietnam. *Sci. Rep.* **8**, 11437 (2018).
17. S.-Y. Yu, T. E. Törnqvist, P. Hu, Quantifying Holocene lithospheric subsidence rates underneath the Mississippi Delta. *Earth Planet. Sci. Lett.* **331-332**, 21–30 (2012).
18. T. E. Törnqvist, J. L. González, L. A. Newsom, K. van der Borg, A. F. M. de Jong, C. W. Kurnik, Deciphering Holocene sea-level history on the U.S. Gulf Coast: A high-resolution record from the Mississippi Delta. *GSA Bull.* **116**, 1026–1039 (2004).
19. J. L. González, T. E. Törnqvist, A new Late Holocene sea-level record from the Mississippi Delta: Evidence for a climate/sea level connection? *Quat. Sci. Rev.* **28**, 1737–1749 (2009).
20. M. Oppenheimer, B. C. Glavovic, J. Hinkel, R. van de Wal, A. K. Magnan, A. Abd-Elgawad, R. Cai, M. Cifuentes-Jara, R. M. DeConto, T. Ghosh, J. Hay, F. Isla, B. Marzeion, B. Meyssignac, Z. Sebesvari, in *IPCC Special Report on the Ocean and Cryosphere in a Changing Climate*, H.-O. Pörtner, D. C. Roberts, V. Masson-Delmotte, P. Zhai, M. Tignor, E. Poloczanska, K. Mintenbeck, A. Alegría, M. Nicolai, A. Okem, J. Petzold, B. Rama, N. Weyer, Eds. (Cambridge Univ. Press, 2019), pp. 321–445.
21. M. Wolstencroft, Z. Shen, T. E. Törnqvist, G. A. Milne, M. Kulp, Understanding subsidence in the Mississippi Delta region due to sediment, ice, and ocean loading: Insights from geophysical modeling. *J. Geophys. Res. Solid Earth* **119**, 3838–3856 (2014).
22. S. van Asselen, The contribution of peat compaction to total basin subsidence: Implications for the provision of accommodation space in organic-rich deltas. *Basin Research* **23**, 239–255 (2011).
23. F. Falcini, N. S. Khan, L. Macelloni, B. P. Horton, C. B. Lutken, K. L. McKee, R. Santoleri, S. Colella, C. Li, G. Volpe, M. D'Emidio, A. Salusti, D. J. Jerolmack, Linking the historic 2011 Mississippi River flood to coastal wetland sedimentation. *Nat. Geosci.* **5**, 803–807 (2012).
24. M. D. Blum, H. H. Roberts, Drowning of the Mississippi Delta due to insufficient sediment supply and global sea-level rise. *Nat. Geosci.* **2**, 488–491 (2009).
25. D. F. Hill, S. D. Griffiths, W. R. Peltier, B. P. Horton, T. E. Törnqvist, High-resolution numerical modeling of tides in the western Atlantic, Gulf of Mexico, and Caribbean Sea during the Holocene. *J. Geophys. Res.* **116**, C10014 (2011).
26. J. A. Langley, K. L. McKee, D. R. Cahoon, J. A. Cherry, J. P. Megonigal, Elevated CO$_2$ stimulates marsh elevation gain, counterbalancing sea-level rise. *Proc. Natl. Acad. Sci. U.S.A.* **106**, 6182–6186 (2009).

27. T. E. Törnqvist, D. J. Wallace, J. E. A. Storms, J. Wallinga, R. L. van Dam, M. Blaauw, M. S. Derksen, C. J. W. Klerks, C. Meijneken, E. M. A. Snijders, Mississippi Delta subsidence primarily caused by compaction of Holocene strata. *Nat. Geosci.* **1**, 173–176 (2008).

28. T. A. Meckel, U. S. Ten Brink, S. J. Williams, Current subsidence rates due to compaction of Holocene sediments in southern Louisiana. *Geophys. Res. Lett.* **33**, L11403 (2006).

29. A. C. Ortiz, S. Roy, D. A. Edmonds, Land loss by pond expansion on the Mississippi River Delta Plain. *Geophys. Res. Lett.* **44**, 3635–3642 (2017).

30. C. A. Wilson, M. A. Allison, An equilibrium profile model for retreating marsh shorelines in southeast Louisiana. *Estuar. Coast. Shelf Sci.* **80**, 483–494 (2008).

31. G. Mariotti, S. Fagherazzi, Critical width of tidal flats triggers marsh collapse in the absence of sea-level rise. *Proc. Natl. Acad. Sci. U.S.A.* **110**, 5353–5356 (2013).

32. B. P. Horton, I. Shennan, S. L. Bradley, N. Cahill, M. Kirwan, R. E. Kopp, T. A. Shaw, Predicting marsh vulnerability to sea-level rise using Holocene relative sea-level data. *Nat. Commun.* **9**, 2687 (2018).

33. J. P. Donnelly, M. D. Bertness, Rapid shoreward encroachment of salt marsh cordgrass in response to accelerated sea-level rise. *Proc. Natl. Acad. Sci. U.S.A.* **98**, 14218–14223 (2001).

34. P. U. Clark, J. D. Shakun, S. A. Marcott, A. C. Mix, M. Eby, S. Kulp, A. Levermann, G. A. Milne, P. L. Pfister, B. D. Santer, D. P. Schrag, S. Solomon, T. F. Stocker, B. H. Strauss, A. J. Weaver, R. Winkelmann, D. Archer, E. Bard, A. Goldner, K. Lambeck, R. T. Pierrehumbert, G.-K. Plattner, Consequences of twenty-first-century policy for multi-millennial climate and sea-level change. *Nat. Clim. Chang.* **6**, 360–369 (2016).

35. Y.-X. Li, T. E. Törnqvist, J. M. Nevitt, B. Kohl, Synchronizing a sea-level jump, final Lake Agassiz drainage, and abrupt cooling 8200 years ago. *Earth Planet. Sci. Lett.* **315-316**, 41–50 (2012).

36. R. Love, G. A. Milne, L. Tarasov, S. E. Engelhart, M. P. Hijma, K. Latychev, B. P. Horton, T. E. Törnqvist, The contribution of glacial isostatic adjustment to projections of sea-level change along the Atlantic and Gulf coasts of North America. *Earths Future* **4**, 440–464 (2016).

37. W. R. Gehrels, P. L. Woodworth, When did modern rates of sea-level rise start? *Glob. Planet. Chang.* **100**, 263–277 (2013).

38. A. S. Kolker, M. A. Allison, S. Hameed, An evaluation of subsidence rates and sea-level variability in the northern Gulf of Mexico. *Geophys. Res. Lett.* **38**, L21404 (2011).

39. E. Oele, W. Apon, M. M. Fischer, R. Hoogendoorn, C. S. Mesdag, E. F. J. de Mulder, B. Overzee, A. Sesören, W. E. Westerhoff, Surveying The Netherlands: Sampling techniques, maps and their applications. *Geologie en Mijnbouw* **62**, 355–372 (1983).

40. H. N. Fisk, E. McFarlan Jr., Late Quaternary deltaic deposits of the Mississippi River. *Geol. Soc. Am. Spec. Pap.* **62**, 279–302 (1955).

41. D. J. Stanley, A. G. Warne, Worldwide initiation of Holocene marine deltas by deceleration of sea-level rise. *Science* **265**, 228–231 (1994).

42. J. M. Coleman, Ecological changes in a massive fresh-water clay sequence. *Gulf Coast Assoc. Geol. Soc. Trans.* **16**, 159–174 (1966).

43. C. R. Kolb, J. R. Van Lopik, in *Deltas in their Geologic Framework,* M. L. Shirley, Ed. (Houston Geological Society, 1966), pp. 17–61.

44. J. M. Coleman, S. M. Gagliano, Sedimentary structures: Mississippi River deltaic plain. *Soc. Econ. Paleontol. Mineral. Spec. Pub.* **12**, 133–148 (1965).

45. R. T. Saucier, *Geomorphology and Quaternary Geologic History of the Lower Mississippi Valley* (Mississippi River Commission, 1994), 364 pp.

46. Soil Survey Staff, *Soil Taxonomy. A Basic System of Soil Classification for Making and Interpreting Soil Surveys* (United States Department of Agriculture, Natural Resources Conservation Service, 1999), 871 pp.

47. L. Vetter, B. E. Rosenheim, A. Fernandez, T. E. Törnqvist, Short organic carbon turnover time and narrow ^{14}C age spectra in early Holocene wetland paleosols. *Geochem. Geophys. Geosyst.* **18**, 142–155 (2017).

48. C. Craft, S. Broome, C. Campbell, Fifteen years of vegetation and soil development after brackish-water marsh creation. *Restoration Ecology* **10**, 248–258 (2002).

49. G. D. Steyer, C. E. Sasser, J. M. Visser, E. M. Swenson, J. A. Nyman, R. C. Raynie, A proposed coast-wide reference monitoring system for evaluating wetland restoration trajectories in Louisiana. *Environ. Monit. Assess.* **81**, 107–117 (2003).

50. M. P. Hijma, S. E. Engelhart, T. E. Törnqvist, B. P. Horton, P. Hu, D. F. Hill, in *Handbook of Sea-Level Research,* I. Shennan, A. J. Long, B. P. Horton, Eds. (John Wiley, 2015), pp. 536–553.

Citation: T. E. Törnqvist, K. L. Jankowski, Y.-X. Li, J. L. González, Tipping points of Mississippi Delta marshes due to accelerated sea-level rise. *Sci. Adv.* **6**, eaaz5512 (2020).

Science Advances

Tipping points of Mississippi Delta marshes due to accelerated sea-level rise

Torbjörn E. Törnqvist, Krista L. Jankowski, Yong-Xiang Li and Juan L. González

Use of this article is subject to the Terms of Service